Coexistence of Ferromagnetic and Stripe-Type Antiferromagnetic Spin Fluctuations in YFe_2Ge_2

Hongliang Wo,[1] Qisi Wang,[1] Yao Shen,[1] Xiaowen Zhang,[1] Yiqing Hao,[1] Yu Feng,[1] Shoudong Shen,[1] Zheng He,[1] Bingying Pan,[1] Wenbin Wang,[2] K. Nakajima,[3] S. Ohira-Kawamura,[3] P. Steffens,[4] M. Boehm,[4] K. Schmalzl,[5] T. R. Forrest,[6] M. Matsuda,[7] Yang Zhao,[8,9] J. W. Lynn,[8] Zhiping Yin,[10] and Jun Zhao[1,11,*]

[1]*State Key Laboratory of Surface Physics and Department of Physics, Fudan University, Shanghai 200433, China*
[2]*Institute of Nanoelectronic Devices and Quantum Computing, Fudan University, Shanghai 200433, China*
[3]*Materials and Life Science Division, J-PARC Center, Tokai, Ibaraki 319-1195, Japan*
[4]*Institut Laue-Langevin, 71 Avenue des Martyrs, 38042 Grenoble Cedex 9, France*
[5]*Forschungszentrum Jülich GmbH. Jülich Centre for Neutron Science at ILL, 71 Avenue des Martyrs, 38000 Grenoble, France*
[6]*Diamond Light Source, Harwell Campus, Didcot OX11 0DE, United Kingdom*
[7]*Neutron Scattering Division, Oak Ridge National Laboratory, Oak Ridge, Tennessee 37831, USA*
[8]*NIST Center for Neutron Research, National Institute of Standards and Technology, Gaithersburg, Maryland 20899, USA*
[9]*Department of Materials Science and Engineering, University of Maryland, College Park, Maryland 20742, USA*
[10]*Department of Physics and Center for Advanced Quantum Studies, Beijing Normal University, Beijing 100875, China*
[11]*Collaborative Innovation Center of Advanced Microstructures, Nanjing, 210093, China*

(Received 6 August 2018; revised manuscript received 2 April 2019; published 31 May 2019)

We report neutron scattering measurements of single-crystalline YFe_2Ge_2 in the normal state, which has the same crystal structure as the 122 family of iron pnictide superconductors. YFe_2Ge_2 does not exhibit long-range magnetic order but exhibits strong spin fluctuations. Like the iron pnictides, YFe_2Ge_2 displays anisotropic stripe-type antiferromagnetic spin fluctuations at $(\pi, 0, \pi)$. More interesting, however, is the observation of strong spin fluctuations at the *in-plane ferromagnetic* wave vector $(0, 0, \pi)$. These ferromagnetic spin fluctuations are isotropic in the (H, K) plane, whose intensity exceeds that of stripe spin fluctuations. Both the ferromagnetic and stripe spin fluctuations remain gapless down to the lowest measured energies. Our results naturally explain the absence of magnetic order in YFe_2Ge_2 and also imply that the ferromagnetic correlations may be a key ingredient for iron-based materials.

DOI: 10.1103/PhysRevLett.122.217003

Spin fluctuations can provide the pairing force for magnetic unconventional superconductors. In cuprate superconductors, it is widely believed that the pairing symmetry is ubiquitously d wave, which is likely mediated by Néel spin fluctuations near (π, π) (square lattice unit cell) [1]. In iron-based superconductors containing both electron and hole Fermi surfaces, enormous previous efforts have been devoted to study the stripe spin fluctuations at $(\pi, 0)$, which tend to result in a sign-reversed s-wave pairing [2]. Interestingly, recent nuclear magnetic resonance (NMR) studies based on the analysis of the modified Korringa relation have suggested the coexistence of antiferromagnetic and ferromagnetic spin correlations in several iron-based superconductors [3], indicating that their magnetism could be more complicated than previously expected. However, ferromagnetic spin fluctuations associated with the FeAs/Se layer have thus far not been confirmed by inelastic neutron scattering experiments in any iron-based superconductor.

The recent discovery of superconductivity in the iron-germanide compound YFe_2Ge_2 ($T_c \sim 1.8$ K), which does not belong to the iron pnictide or chalcogenide families, provides a new opportunity to investigate the nature of spin fluctuations and their possible link with superconductivity in iron-based materials [4,5]. YFe_2Ge_2 has the same layered crystal structure to the 122 family of iron pnictides, namely, the $ThCr_2Si_2$-type structure, but possesses a shorter interlayer distance [6]. Nevertheless, angle-resolved photoemission spectroscopy (ARPES) has revealed a quasi-two-dimensional electronic structure with two hole pockets at the zone center and one electron pocket at the zone edge in YFe_2Ge_2 [7], which is similar to that of 122 iron pnictides. Density functional theory calculations predict an in-plane ferromagnetic ordered state in YFe_2Ge_2 [8,9], resembling its sister compound $LuFe_2Ge_2$ [10]. However, no indication of any magnetic phase transition was observed by thermodynamic measurements down to the lowest measured temperature in YFe_2Ge_2 [4,5,11]. Instead, evidence for fluctuating magnetic moments in the core-level photoemission spectroscopy measurements indicates the system is close to magnetic instabilities [12]. Moreover, NMR measurements suggested the coexistence of antiferromagnetic and ferromagnetic spin fluctuations in polycrystalline $YFe_2(Ge, Si)_2$ [13]. These results together with the non-Fermi-liquid behavior of the resistivity and specific heat and the

extremely disorder-sensitive superconductivity favor an unconventional pairing mechanism [4,5,14]. Indeed, theoretical studies have proposed several unconventional pairing models, including a singlet pairing with an $s\pm$ gap function mediated through antiferromagnetic fluctuations [8] and a triplet pairing associated with the in-plane ferromagnetic fluctuations [9]. Thus, the elucidation of the nature of the spin fluctuations is pivotal to understanding the magnetism and superconductivity in this class of material.

We use neutron scattering to measure the spin fluctuations in YFe_2Ge_2 single crystals over the entire Brillouin zone. The experiments were carried out on the AMATERAS cold neutron disk chopper spectrometer at the Japan Proton Accelerator Research Complex [15], the ThALES three-axis low-energy spectrometer at the Institut Laue-Langevin, Grenoble, France, the BT-7 triple-axis spectrometer at the NIST Center for Neutron Research [16], and the HB-1 triple-axis spectrometer at the High Flux Isotope Reactor, Oak Ridge National Laboratory. Our YFe_2Ge_2 single crystals were synthesized using the Sn-flux method. The crystals have a platelike shape and show a residual resistivity ratio (RRR) of ~40–60. According to Ref. [5], the samples with RRR between 20 and 70 were nonsuperconducting or partially superconducting; bulk superconductivity was observed only in samples with RRR exceeding 70. This suggests that the superconductivity is extremely sensitive to disorder [5]. Similar behavior has also been observed in the putative triplet p-wave superconductor Sr_2RuO_4 [17]. Nevertheless, our powder x-ray diffraction measurements on ground YFe_2Ge_2 single crystals found a single phase with no evidence of phase separation; the Rietveld refined lattice parameters [18] are consistent with those of bulk superconducting samples in Ref. [5]. We have coaligned around 200 pieces of single crystals with a total mass of 4 g to achieve high counting statistics for the inelastic neutron scattering experiments. Since our measurements were performed in the normal state, the variation in superconducting properties induced by disorder is not expected to affect the spin excitation spectrum significantly, which is commonly the case in magnetic superconductors such as Sr_2RuO_4 [22,23].

Figure 1 shows a contour plot of the spin fluctuations in the (H, K, 0.5) plane at 4 K. Clear scattering appears at $\mathbf{Q} = (0, 0.5, 0.5)$ and equivalent positions, corresponding to the stripe wave vector (1-Fe unit cell). The magnetic scattering is anisotropic in the (H, K) plane and elongates along the longitudinal direction with respect to the reduced momentum transfer $\mathbf{q}$. This behavior resembles that of the hole-doped iron pnictides but differs from that of the electron-doped iron pnictides, in which the scattering pattern is transversely elongated [2]. It should be noted that the nominal electron occupation of YFe_2Ge_2 for Fe is hole-doped $3d^{5.5}$, which seems consistent with the ARPES measurements that revealed two hole pockets at the zone center [7]. However, it was also suggested that the relatively

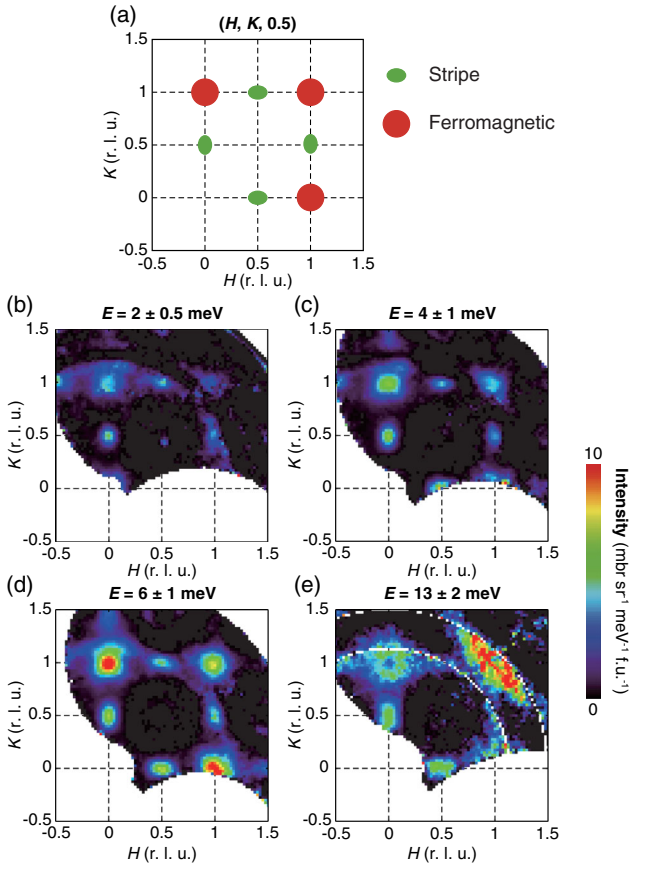

FIG. 1. Momentum dependence of the spin fluctuations in YFe_2Ge_2 at 4 K. (a) Schematic representation of the stripe and ferromagnetic spin fluctuations in the (H, K, 0.5) plane. (b)–(e) Constant-energy images at indicated energies. The measurements (b)–(d) and (e) were carried out on AMATERAS using the incident neutron energies of 15 and 42 meV, respectively. The data were analyzed using the HORACE program [24]. The $|\mathbf{Q}|$-dependent background has been subtracted using a similar method described in Ref. [25]. The intensities are normalized to absolute units with acoustic phonons.

short Ge-Ge distance along the c axis may lead to covalent bonds between Ge ions $[\text{Ge-Ge}]^{6-}$ [8]; the corresponding electron occupation of Fe, therefore, becomes electron-doped $3d^{6.5}$. It will be interesting to determine the exact electron concentration of YFe_2Ge_2 to see whether or how it can fit into the phase diagram of the carrier-doped 122 iron pnictides. More notably, in addition to the in-plane stripe-type antiferromagnetic spin fluctuations, much stronger spin responses are observed at $\mathbf{Q} = (0, 1, 0.5)$ and equivalent positions (Fig. 1), corresponding to the in-plane ferromagnetic wave vector. In contrast to the anisotropic stripe spin fluctuations, the ferromagnetic spin fluctuations are nearly isotropic along the H and K directions. With increasing energy, the ferromagnetic fluctuations disperse outwards, forming a nearly isotropic ring at 13 meV. The signals at both the stripe wave vector and ferromagnetic wave vector weaken with increasing $|\mathbf{Q}|$ because of the

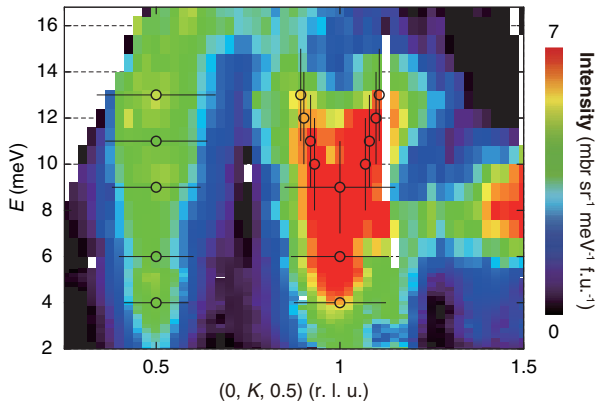

FIG. 2. Dispersions of the stripe ($K \sim 0.5$) and the ferromagnetic spin fluctuations ($K \sim 1$) in YFe_2Ge_2 at 4 K. The low-energy ($E < 5.6$ meV) and the high-energy (5.6 meV $< E <$ 16.8 meV) parts were measured on AMATERAS with incident neutron energies of 15 and 42 meV, respectively. The $|\mathbf{Q}|$-dependent background subtraction and intensities normalization were performed in the same way as in Fig. 1. The open circles represent for the peak positions determined from the Gaussian fitting of the constant-energy scans. The horizontal bars show the full width at half maximum (FWHM) of the peaks, while the vertical bars indicate the range of integrated energies.

reduced magnetic form factor, indicating their magnetic origin. This is further confirmed by the polarization analysis of the constant-energy scans [18]. On the other hand, no magnetic Bragg peaks at either the stripe or ferromagnetic wave vector were observed at temperatures down to 2 K (not shown), suggesting the magnetic ground state exhibits only spin fluctuations.

In order to elucidate the dispersion of the spin fluctuations, we present E-$\mathbf{Q}$ relationships in Fig. 2. The stripe spin fluctuations exhibit a conelike dispersion in the projection along the K direction [or, equivalently, the H directions for the (0.5, 0, 0.5) peak], consistent with the constant-energy scans in Fig. 3. The scans along the longitudinal and transverse directions at the stripe wave vector are anisotropic [Figs. 3(a)–3(l)], with a shorter dynamical spin correlation length along the longitudinal direction [Figs. 3(g)–3(l)] versus a steeper dispersion and longer correlation length along the transverse direction [Figs. 3(a)–3(f)]. This further confirms the anisotropy of the stripe spin fluctuation seen in the constant-energy images in Fig. 1.

As for the ferromagnetic fluctuations, two branches of scattering arising from (0, 1, 0.5) can be clearly observed (Fig. 2). This can be illustrated more quantitatively in Figs. 3(m)–3(r). At $E = 2$ meV, a well-defined peak occurs centered at the ferromagnetic wave vector, which is broadened and then evolves into a pair of peaks with increasing energy. The peak positions and peak widths are determined by fitting the constant-energy scans with Gaussian profiles [Figs. 3(a)–3(r)], which are consistent with the contour plot in Fig. 2. We attempted but failed to fit the whole spectrum using a linear spin-wave theory for the

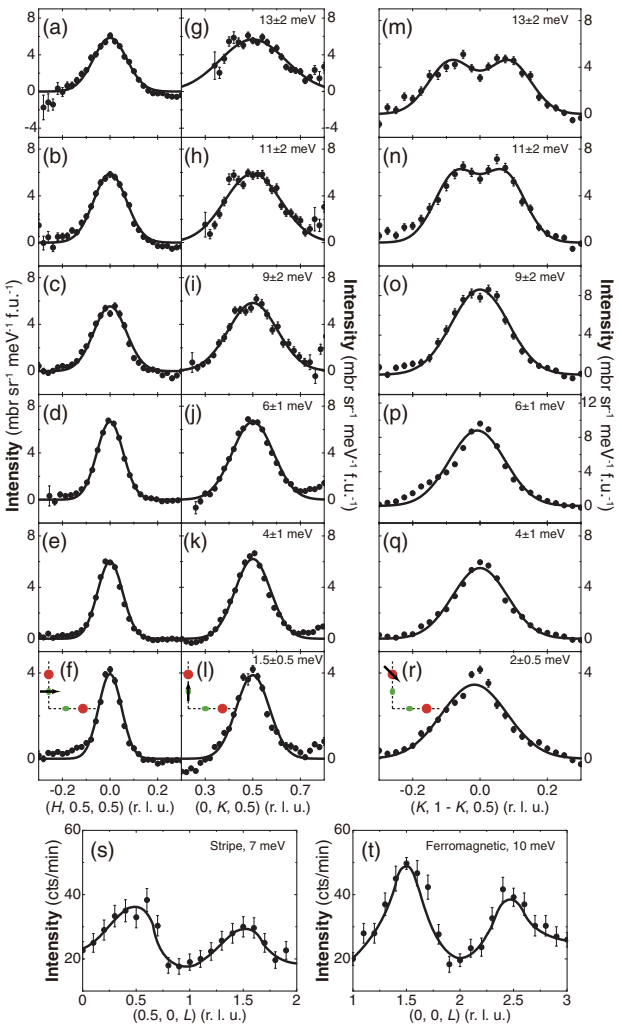

FIG. 3. Constant-energy scans of the stripe and ferromagnetic spin fluctuations in YFe_2Ge_2 at 4 K. (f) and (l), [(d), (e), (j), (k), and (p)–(r)], and [(a)–(c), (g)–(i), and (m)–(o)] were collected on AMATERAS with the incident neutron energies of 8, 15, and 42 meV, respectively. (s) and (t) were measured on the HB-1 triple-axis spectrometer. (a)–(f) Background subtracted constant-energy scans through the stripe spin fluctuation along the H (transverse) direction. (g)–(l) Background subtracted constant-energy scans for the stripe spin fluctuation along the K (longitudinal) direction. (m)–(r) Background subtracted constant-energy scans for the in-plane ferromagnetic spin fluctuation along the (K, 1-K) direction. (s),(t) Constant-energy scans along the L direction for the stripe and the in-plane ferromagnetic spin fluctuations.

Heisenberg model in either a pure stripe-type or a pure in-plane ferromagnetic order, because neither of them can account for the observed strong spin excitations at both wave vectors. The spin correlations along the c axis are illustrated by constant-energy scans along the L direction in Figs. 3(s) and 3(t), where a clear L modulation of the scattering intensity is observed. Such behavior is commonly seen in 122 iron pnictides where the interlayer coupling is not negligible. Both the stripe and ferromagnetic spin fluctuation

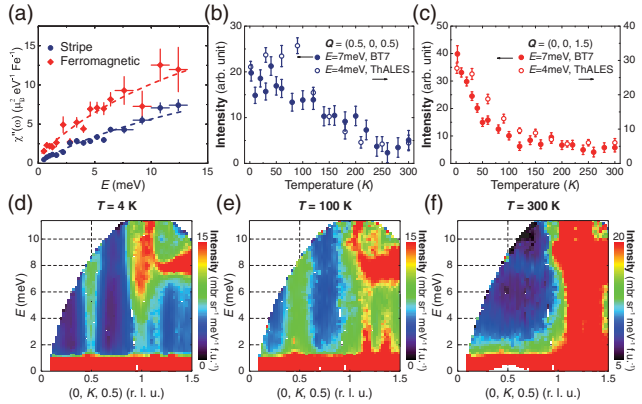

FIG. 4. Momentum-integrated local susceptibility and temperature dependence of the stripe and ferromagnetic spin fluctuations in YFe_2Ge_2. (a) $\chi''(\omega)$ of the stripe and ferromagnetic spin fluctuations in YFe_2Ge_2 at 4 K. The absolute units were obtained via normalization for the acoustic phonon mode. (b),(c) The $E = 4$ meV data (open circles) and the $E = 7$ meV (filled circles) were collected on ThALES and BT-7, respectively. The error bars indicate one standard deviation. (d)–(f) Raw data for the E-$\mathbf{Q}$ relationship at different temperatures. The data were measured on AMATERAS with the incident neutron energy of 15 meV.

spectra exhibit a maximum intensity at $L = 0.5, 1.5, 2.5, \ldots$, indicating an antiferromagnetic interlayer coupling, which is consistent with the density functional theory calculations [8,9].

By normalizing the spin excitation intensities with acoustic phonon modes [26], we can calculate the momentum-integrated local susceptibility $\chi''(\omega)$ in absolute units. Figure 4(a) shows that the ferromagnetic spectral weight between 0.5 and 12.4 meV is about 1.8 times larger than that of the stripe spin excitations, implying that the system could be closer to ferromagnetic order than stripe order. Both the ferromagnetic and stripe spin fluctuations remain gapless down to the lowest measured energy (0.5 meV) [Fig. 4(a)]. We note that the total local susceptibility in YFe_2Ge_2 is comparable to that of 122 iron pnictides at the energies measured [2]. This is not surprising, since both systems have similar strength of electron correlations [7].

More insight into the nature of these two types of spin fluctuations can be obtained by measuring their temperature dependence. As is shown in Fig. 4(b), the intensity of the stripe spin fluctuations shows a gradual decrease with increasing temperature from 4 to 300 K. Such behavior is consistent with its magnetic origin and resembles the low-energy response in other iron-based superconductors [27]. On the other hand, warming from a low temperature, the ferromagnetic spin fluctuations exhibit a steeper reduction with the correlations becoming negligible above ~200 K [Fig. 4(b)]. The different temperature dependence of spin fluctuations could be due to the competition between these two magnetic instabilities; the ferromagnetic instability is favored at a low temperature (4 K), while the stripe spin fluctuations is more stable against thermal fluctuations at a relatively higher temperature (>200 K). This is further confirmed by the E-$\mathbf{Q}$ slices at various temperatures, where ferromagnetic spin fluctuations disappear more rapidly with an increasing temperature [Figs. 4(d)–4(f)]. On the other hand, the intensity of the phonon scattering at large q increases significantly on warming because of the Bose population factor.

The unambiguous observation of stripe and ferromagnetic spin fluctuations within the Fe plane in one compound has important implications for understanding the nature of the magnetism and superconductivity in iron-based superconductors. Although density functional theory calculations and NMR measurements have suggested the coexistence of ferromagnetic and antiferromagnetic correlations in several classes of iron-based superconductors [3,8,9,13,28–31], YFe_2Ge_2 is the first compound in which ferromagnetic spin fluctuations are observed in inelastic neutron scattering experiments. Ferromagnetic fluctuations, in general, tend to mediate p-wave triplet pairing and introduce pair breaking for singlet superconductivity, while antiferromagnetic fluctuations behave in an opposite manner [9]. In this sense, the observation of stronger ferromagnetic spin fluctuations seems to favor a triplet pairing, while singlet pairing associated with stripe spin fluctuations could be a competitor. Regardless of the pairing symmetry, this may account for the relatively low T_c in YFe_2Ge_2, since neither the ferromagnetic nor stripe spin fluctuation is completely dominating. To accurately determine the pairing symmetry, detailed microscopic measurements of the superconducting gap structure in the superconducting state are required.

The competition of the ferromagnetic and the stripe magnetic instabilities also provides a natural understanding of the absence of magnetic order in YFe_2Ge_2. This is in analogy to FeSe, where the stripe spin fluctuations coexist with the Néel spin fluctuations [25], resulting in a frustrated nematic ground state. However, in contrast to FeSe, where nematic order develops at ~90 K, no evidence for nematicity has been revealed so far in YFe_2Ge_2. This could be due to the fact that ferromagnetic fluctuations are stronger in YFe_2Ge_2 while nematicity is generally coupled with stripe spin fluctuations. We note that electron doping or applying pressure in FeSe may partially remove the magnetic frustration and significantly enhance T_c [25,32–36]. It therefore would be interesting to see if doping or pressure can do the same in YFe_2Ge_2.

In summary, we have presented a neutron scattering study of spin correlations of YFe_2Ge_2 single crystals. Unlike previous neutron studies focusing on antiferromagnetic spin fluctuations in iron pnictides or chalcogenides, we find the coexistence of strong stripe and ferromagnetic spin fluctuations within the Fe plane in YFe_2Ge_2, which suggests that it is a competition between the two that determines the fluctuating magnetic ground state and its relation to the pairing mechanism. By determining the

momentum-integrated magnetic spectral weight in absolute units, we show that the ferromagnetic spin fluctuations are stronger than stripe spin fluctuations in the low-temperature regime, which possibly points to an unconventional triplet pairing. Our results, together with reported NMR data [3,13], imply that the competition between ferromagnetic and antiferromagnetic spin fluctuations could be a general property of iron-based superconductors and call for a detailed search for the ferromagnetic correlations in other iron-based superconductors.

We thank J. T. Park for the assistance with the ThALES experiment and D. F. Xu and D. L. Feng for discussions. This work was supported by the Innovation Program of Shanghai Municipal Education Commission (Grant No. 2017-01-07-00-07-E00018), the Ministry of Science and Technology of China (Program 973: 2015CB921302), and the National Key R&D Program of the MOST of China (Grant No. 2016YFA0300203). A portion of this research used resources at the High Flux Isotope Reactor, a Department of Energy Office of Science User Facility operated by the Oak Ridge National Laboratory. The experiment at AMATERAS was carried out under approval of J-PARC Center (Proposal No. 2015A0126).

H. W., Q. W., and Y. S. contributed equally to this work.

*To whom all correspondence should be addressed.
zhaoj@fudan.edu.cn

[1] P. A. Lee, N. Nagaosa, and X. G. Wen, Rev. Mod. Phys. **78**, 17 (2006).
[2] P. C. Dai, Rev. Mod. Phys. **87**, 855 (2015).
[3] P. Wiecki, B. Roy, D. C. Johnston, S. L. Bud'ko, P. C. Canfield, and Y. Furukawa, Phys. Rev. Lett. **115**, 137001 (2015).
[4] Y. Zou, Z. Feng, P. W. Logg, J. Chen, G. I. Lampronti, and F. M. Grosche, Phys. Status Solidi RRL **8**, 928 (2014).
[5] J. S. Chen, K. Semeniuk, Z. Feng, P. Reiss, P. Brown, Y. Zou, P. W. Logg, G. I. Lampronti, and F. M. Grosche, Phys. Rev. Lett. **116**, 127001 (2016).
[6] G. Venturini and B. Malaman, J. Alloys Compd. **235**, 201 (1996).
[7] D. F. Xu *et al.*, Phys. Rev. B **93**, 024506 (2016).
[8] A. Subedi, Phys. Rev. B **89**, 024504 (2014).
[9] D. J. Singh, Phys. Rev. B **89**, 024505 (2014).
[10] T. Fujiwara, N. Aso, H. Yamamoto, M. Hedo, Y. Saiga, M. Nishi, Y. Uwatoko, and K. Hirota, J. Phys. Soc. Jpn. **76**, 60 (2007).
[11] M. A. Avila, S. L. Bud'Ko, and P. C. Canfield, J. Magn. Magn. Mater. **270**, 51 (2004).
[12] N. Sirica, F. Bondino, S. Nappini, I. Píš, L. Poudel, A. D. Christianson, D. Mandrus, D. J. Singh, and N. Mannella, Phys. Rev. B **91**, 121102(R) (2015).
[13] J. Srpčič, P. Jeglič, I. Felner, B. Lv, C. W. Chu, and D. Arčon, Phys. Rev. B **96**, 174430 (2017).
[14] H. Kim, S. Ran, E. D. Mun, H. Hodovanets, M. A. Tanatar, R. Prozorov, S. L. Bud'ko, and P. C. Canfield, Philos. Mag. **95**, 804 (2015).
[15] K. Nakajima *et al.*, J. Phys. Soc. Jpn. **80**, SB028 (2011).
[16] J. W. Lynn, Y. Chen, S. Chang, Y. Zhao, S. Chi, W. Ratcliff II, B. G. Ueland, and R. W. Erwin, J. Res. Natl. Inst. Stand. Technol. **117**, 61 (2012).
[17] A. P. Mackenzie and Y. Maeno, Rev. Mod. Phys. **75**, 657 (2003).
[18] See Supplemental Material at http://link.aps.org/supplemental/10.1103/PhysRevLett.122.217003 for sample characterizations, simulated spin excitation spectrum, raw data, and additional polarized neutron scattering data, which includes Refs. [5,16,19–21].
[19] J. Rodrguez-Carvajal, Physica (Amsterdam) **192B**, 55 (1993).
[20] W. C. Chen, G. Armstrong, Y. Chen, B. Collett, R. Erwin, T. R. Gentile, G. L. Jones, J. W. Lynn, S. McKenney, and J. E. Steinberg, Physica (Amsterdam) **397B**, 168 (2007).
[21] S. Toth and B. Lake, J. Phys. Condens. Matter **27**, 166002 (2015).
[22] Y. Sidis, M. Braden, P. Bourges, B. Hennion, S. NishiZaki, Y. Maeno, and Y. Mori, Phys. Rev. Lett. **83**, 3320 (1999).
[23] M. Braden, Y. Sidis, P. Bourges, P. Pfeuty, J. Kulda, Z. Mao, and Y. Maeno, Phys. Rev. B **66**, 064522 (2002).
[24] R. A. Ewings, A. Buts, M. D. Le, J. van Duijn, I. Bustinduy, and T. G. Perring, Nucl. Instrum. Methods Phys. Res., Sect. A **834**, 132 (2016).
[25] Q. S. Wang *et al.*, Nat. Commun. **7**, 12182 (2016).
[26] G. Y. Xu, Z. J. Xu, and J. M. Tranquada, Rev. Sci. Instrum. **84**, 083906 (2013).
[27] Q. S. Wang *et al.*, Nat. Mater. **15**, 159 (2016).
[28] D. J. Singh and M. H. Du, Phys. Rev. Lett. **100**, 237003 (2008).
[29] I. I. Mazin, D. J. Singh, M. D. Johannes, and M. H. Du, Phys. Rev. Lett. **101**, 057003 (2008).
[30] J. Dong *et al.*, Europhys. Lett. **83**, 27006 (2008).
[31] D. Guterding, H. O. Jeschke, I. I. Mazin, J. K. Glasbrenner, E. Bascones, and R. Valentí, Phys. Rev. Lett. **118**, 017204 (2017).
[32] S. Medvedev *et al.*, Nat. Mater. **8**, 630 (2009).
[33] Q. Y. Wang *et al.*, Chin. Phys. Lett. **29**, 037402 (2012).
[34] B. Y. Pan *et al.*, Nat. Commun. **8**, 123 (2017).
[35] Y. Miyata, K. Nakayama, K. Sugawara, T. Sato, and T. Takahashi, Nat. Mater. **14**, 775 (2015).
[36] B. Lei, J. H. Cui, Z. J. Xiang, C. Shang, N. Z. Wang, G. J. Ye, X. G. Luo, T. Wu, Z. Sun, and X. H. Chen, Phys. Rev. Lett. **116**, 077002 (2016).

Supplementary Materials: Coexistence of ferromagnetic and stripe spin fluctuations in YFe_2Ge_2

I. X-ray diffraction measurements

YFe_2Ge_2 single crystals were grown out of Sn flux. Representative single crystals with shiny cleaved surfaces are shown in Fig. S1a. X-ray diffraction (XRD) measurements revealed that all of the reflections from the cleaved surface could be indexed by (0, 0, *L*) peaks of tetragonal YFe_2Ge_2 (Fig. S1b). The full-width at half maximum (FWHM) of the rocking curve of the (0, 0, 8) peak was 0.073° (Fig. S1c), indicating a high crystallization quality. The Rietveld refinements on the X-ray powder diffraction pattern of the ground single crystals found no detectable impurity phases (Fig. S1d). The refined structural parameters are listed in Table S1, which are consistent with previous reports [1].

II. Raw constant energy images measured on the AMATERAS time of flight spectrometer

Fig. S2 shows the raw constant energy images at 4 K, in which the stripe and the in-plane ferromagnetic spin fluctuations can be clearly seen. An aluminum sample holder/environment was used for our neutron scattering measurements. The phonon background from the polycrystalline aluminum sample holder/environment only depends on the amplitude of **Q**, which was estimated from the scattering away from the magnetic signals and subtracted. The background-subtracted images are presented in Fig. 1.

III. Polarized inelastic neutron scattering measurements on YFe_2Ge_2

In order to unambiguously confirm that the stripe and the ferromagnetic spin excitations are magnetic, we have performed polarized neutron scattering measurements on BT-7 triple-axis spectrometer at the NIST Center for Neutron Research [3, 4]. Typical initial flipping ratio in the experiment was ~ 25 and small corrections for the polarization inefficiencies have been applied. Fig. S3a illustrates the constant energy scan along the *H* direction around the ferromagnetic wave vector (0, 0, 1.5) and the stripe wave vector (0.5, 0, 1.5) with the neutron polarization direction, controlled by a small guide field, parallel to the momentum transfer **Q** (defined as x). In this configuration, all magnetic signals appear in the spin-flip (SF) channel

and the non-spin-flip (NSF) channel contains only the structural contributions. The strong and clear peaks are observed in the SF channel for both the ferromagnetic and the stripe spin excitations while the signal in the NSF channel is featureless. These results unambiguously demonstrate that the excitations at the stripe and ferromagnetic wavevectors are purely magnetic. On the other hand, the elastic polarized neutron scattering data at the stripe (0.5, 0, 1.5) and the ferromagnetic (1, 0, 0.5) wavevectors are featureless in the SF channel, indicating the absence of magnetic order in YFe_2Ge_2 at 1.5 K (Fig. S3b and S3c).

IV. Simulated spin excitation spectrum using a linear combination of the stripe model and in-plane ferromagnetic model

Here we try to simulate spin excitation spectrum using a linear combination of the stripe model and in-plane ferromagnetic model, assuming the effective Heisenberg Hamiltonian $H = J_{1a}\sum_{i,j}\mathbf{S}_i \cdot \mathbf{S}_j + J_{1b}\sum_{i,j}\mathbf{S}_i \cdot \mathbf{S}_j + J_2\sum_{i,j}\mathbf{S}_i \cdot \mathbf{S}_j + J_c\sum_{i,j}\mathbf{S}_i \cdot \mathbf{S}_j - J_s\sum_i(S_i^z)^2$ for both two models, in which J_{1a}, J_{1b} and J_c are the nearest neighbour exchange coupling constants, J_2 is the next nearest neighbour coupling constant, J_s is the single ion anisotropy. The dynamic spin structure factor is modelled as $S_{tot} = \eta S_{stripe} + (1 - \eta)S_{ferro}$, representing for a linear combination of the stripe model and in-plane ferromagnetic model, in which η is the linear combination coefficient. Fig. S4 illustrates a representative result of our simulation. The exchange coupling parameters used for simulation for the stripe model are SJ_{1a} = -12.5 meV, SJ_{1b} = -15 meV, SJ_2 = 10 meV, SJ_c = 5 meV; for the ferromagnetic model, $SJ_{1a} = SJ_{1b}$ = -30.5 meV, SJ_2 = 10 meV and SJ_c = 5 meV. The coefficient η is about 0.34, which is the phase fraction for the stripe phase.

TABLE S 1: Refined structure parameters of YFe_2Ge_2 via X-ray powder diffraction measurement at 300 K. Space group: *I*4/mmm (No. 139). Atomic position: Y: 2a (0, 0, 0); Fe: 4d (0, 0.5, 0.25); Ge: 4e (0, 0, z).

	Refined composition	YFe_2Ge_2
	a (Å)	3.95835(9)
	c Å)	10.43385(26)
Y atom	B_{iso} *(Å^2)*	0.069(48)
Fe atom	B_{iso} *(Å^2)*	0.242(57)
Ge atom	*z*	0.37868(14)
	B_{iso} *(Å^2)*	0.009(44)
	R_p	3.30
	wR_p	4.24
	χ^2	1.90

[1] J. S. Chen, K. Semeniuk, Z. Feng, P. Reiss, P. Brown, Y. Zou, P. W. Logg, G. I. Lampronti, and F. M. Grosche, Phys. Rev. Lett. **116**, 127001 (2016).

[2] J. Rodrguez-Carvajal, *Physica(Amsterdam)*, **192B**, 55 (1993).

[3] J. W. Lynn, Y. Chen, S. Chang, Y. Zhao, S. Chi, W. Ratcliff, II, B. G. Ueland, and R. W. Erwin, Journal of Research of NIST **117**, 61-79 (2012).

[4] W. C. Chen, G. Armstrong, Y. Chen, B. Collett, R. Erwin, T. R. Gentile, G. L. Jones, J. W. Lynn, S. McKenney and J. E. Steinberg, *Physica* B, **397**, 168 (2007).

[5] S. Toth and B. Lake, J. Phys.: Condens. Matter **27**, 166002 (2015).

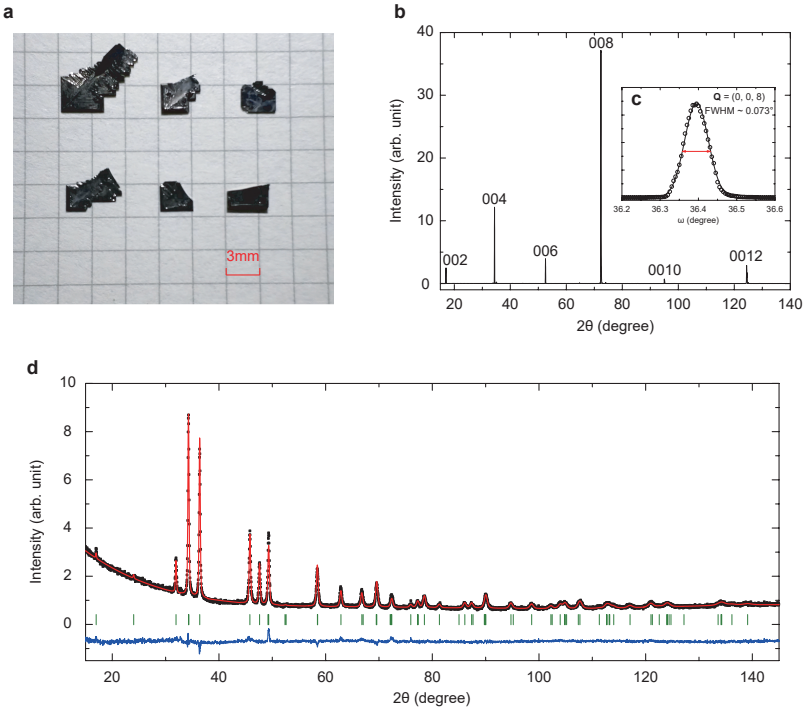

FIG. S 1: Photograph and X-ray diffraction patterns of YFe_2Ge_2. (a) Photograph of representative YFe_2Ge_2 single crystals. (b) X-ray diffraction pattern on YFe_2Ge_2 single crystal. (c) Rocking curve of the (0, 0, 8) reflection peak; the red bar indicates the FWHM. (d) Observed (black) and calculated (red) X-ray diffraction pattern of ground single crystals. The difference between the observed and calculated intensities are shown in the blue curve. Refinements were performed using the FULLPROF program [2]. The X-ray has a wavelength of 1.54 Å.

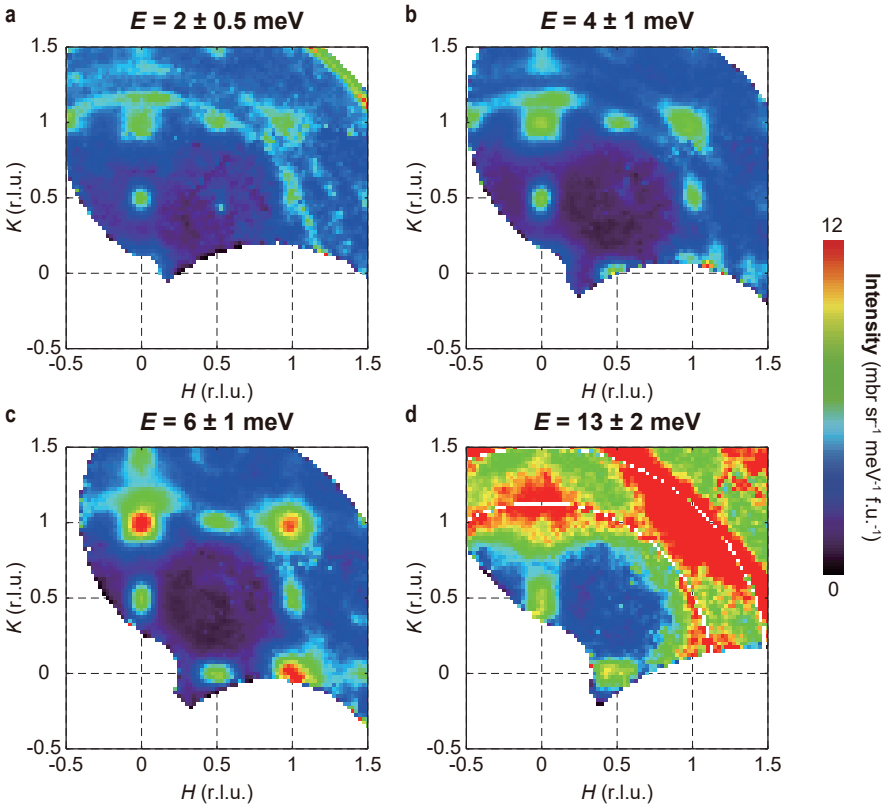

FIG. S 2: Raw constant energy images measured on AMATERAS at indicated energies and 4 K. The corresponding background-subtracted data are shown in Fig. 1b-e.

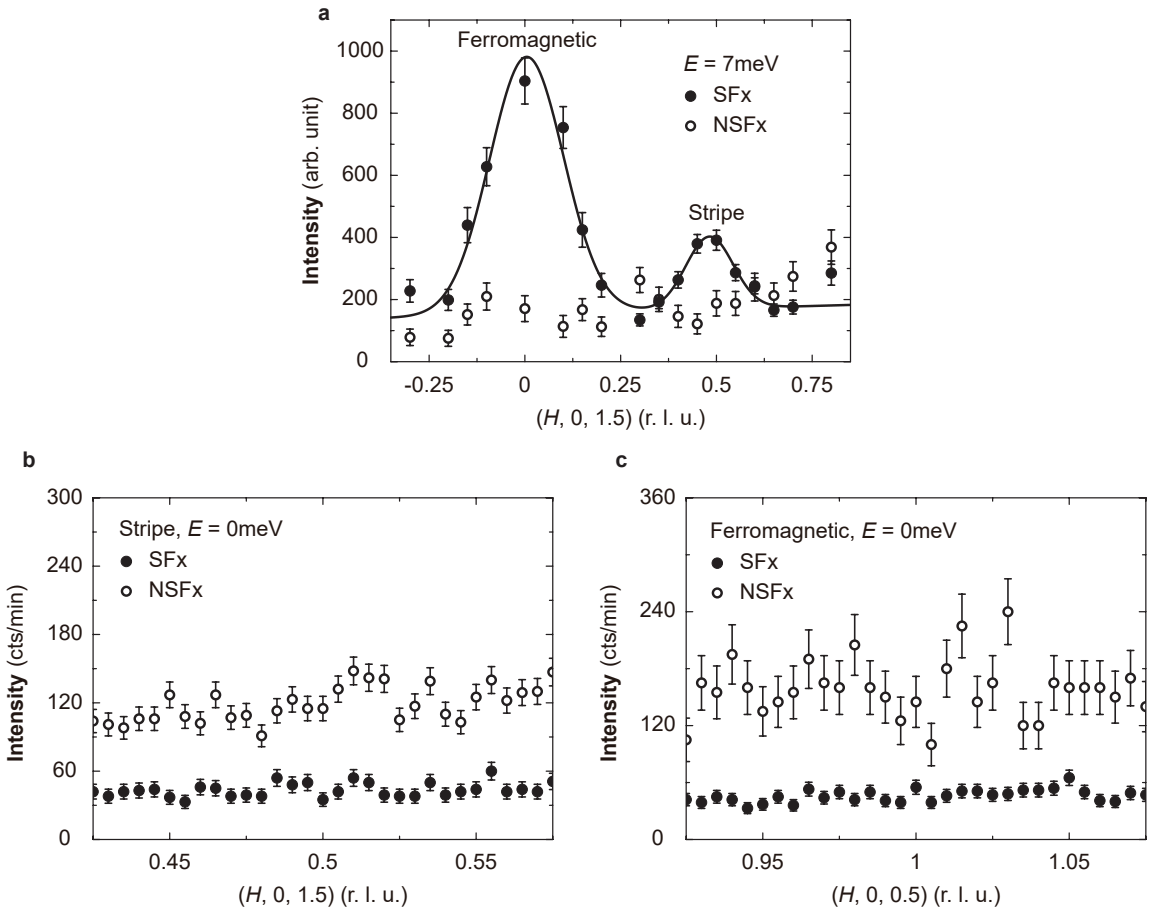

FIG. S 3: Polarized neutron scattering data in the SF and NSF channels at (a) E = 7 meV at the stripe and ferromagnetic wavevectors (b) E = 0 meV at the stripe wavevector (c) E = 0 meV at the ferromagnetic wavevector. The solid line represents for the Gaussian fitting of the spin excitations in the SF channel.

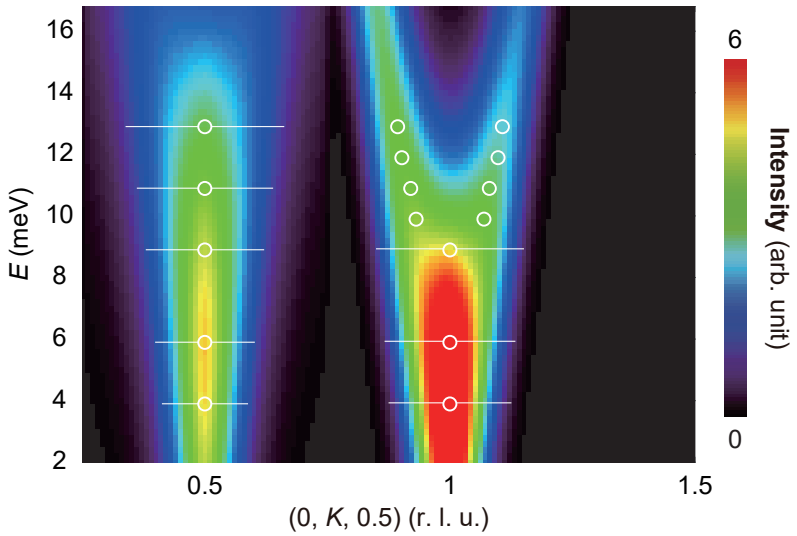

FIG. S 4: The simulated dispersions of the stripe and the ferromagnetic spin excitations in YFe_2Ge_2 using the parameters given in the main text. The open circles and the horizontal bars represent for the peak positions and the full-width at half maximum (FWHM) determined from the experiment results, respectively. The spin excitation spectrum was simulated using the SPINW program [5] for the Heisenberg model.